

screen in the two-phase medium make inverse screens ineffective for decreasing the parameters of shock waves.

LITERATURE CITED

1. L. I. Campbell and A. S. Pitcher, "Shock waves in a liquid containing gas bubbles," Proc. R. Soc., A243, No. 1235 (1958).
2. B. E. Gel'fand, S. A. Gubin, et al., "Investigation of compression waves in a liquid-gas bubble mixture," Dokl. Akad. Nauk SSSR, 213, No. 5 (1973).
3. G. M. Lyakhov and V. N. Okhitin, "Spherical detonation waves in multicomponent media," Zh. Prikl. Mekh. Tekh. Fiz., No. 2 (1974).
4. B. E. Gel'fand, A. V. Gubanov, et al., "Attenuation of shock waves in a two-phase gas-bubble-liquid medium," Izv. Akad. Nauk SSSR, Mekh. Zhidk. Gaza, No. 1 (1977).
5. B. E. Gel'fand, S. A. Gubin, et al., "Passage of shock waves through the separation boundary in two-phased gas-liquid media," Izv. Akad. Nauk SSSR, Mekh. Zhidk. Gaza, No. 6 (1974).
6. B. R. Parkin, F. R. Gilmer, and G. A. Broude, "Shock waves in water with air bubbles," in: Underwater and Underground Explosions [Russian translation], Mir, Moscow (1974).
7. M. Grosely and J. Krivokapic, "Djelovanje eksplozije u vodi," Miniranje, Vol. 8, No. 3 (1976).
8. G. A. Druzhinin, G. A. Ostroumov, and A. S. Tokman, "Nonlinear reflections of shock waves and shock curves for liquids with gas bubbles," in: Nonlinear Stress Waves [in Russian], Tallin (1978).

STRUCTURE OF COMPRESSION AND RAREFACTION WAVES IN A VAN DER WAALS GAS WITH CONSTANT SPECIFIC HEAT

A. A. Borisov and G. A. Khabakhpashev

UDC 532.592+534.222+536.441

It is known [1] that the change in entropy in shocks of weak intensity is proportional to the change in specific volume to the third power: $S_2 - S_1 = (\partial^2 p / \partial V^2) (V_1 - V_2)^3 / 12T_1$, where p is the pressure, V is the specific volume, T is the temperature, and the subscripts 1 and 2 denotes values of the quantities in front of and behind the front, respectively. In an ideal gas, as well as in the majority of actually realizable situations, $(\partial^2 p / \partial V^2)_S > 0$. Therefore, the condition of entropy growth allows the existence of compression shocks and forbids the existence of rarefaction shocks (Zemlen theorem).

However, Zel'dovich [2] has shown that near the fluid-vapor critical point, $(\partial^2 p / \partial V^2)_S$ can be less than zero under definite conditions. In this domain of anomalous thermodynamic properties, compression waves should be spread out in time, while rarefaction waves are propagated in the form of (rare) shocks. A more complex case, in which the unperturbed state is in the domain of anomalous thermodynamic properties while the perturbed state is outside (or conversely), has been considered theoretically in a number of papers, a detailed summary of which is given in [3]. The main attention in these papers is given over to an analysis of the wave adiabats of such media. The question of the existence of exact self-similar solutions of the problem under consideration has not yet been investigated. An evolutionary equation has been obtained in [4] for long-wave perturbations of finite amplitude which can be used to explain the possible multiwave structure of rarefaction waves.

The first experiment to study the propagation of finite-amplitude perturbations in the critical domain was performed on a "shock tube" type apparatus [5]. The rarefaction wave profiles were determined in this experiment, hence it is desirable to obtain the theoretical results also in analogous form. In this connection, the question of the pressure wave structure near the fluid-vapor critical point is investigated in this paper by using a numerical solution of the problem of the dissociation of an arbitrary discontinuity.

1. The behavior of real substances whose state is not in direct proximity to the critical point or in a two-phase domain is described well by the van der Waals model [6]. The van der Waals equation of state is ordinarily written in the form

$$(p + a/V^2)(V - b) = R_G T, \quad (1.1)$$

where a and b are van der Waals constants, $R_G = R/\mu$, R is the universal gas constant, and μ is the molecular mass.

Let the isochoric specific heat C_V be constant. (This assumption is valid in the same domain of parameters where the van der Waals equation is applicable.) We then have for the specific internal energy [7]

$$E = C_V T - a/V. \quad (1.2)$$

Moreover, let us examine the isentropic and shock adiabat equations. The equation of the isentropic adiabat for a van der Waals gas with constant specific heat can be written in the form

$$p^* = (p_0 + 3/v_0^2) [(v_0 - 1/3)/(v - 1/3)]^\gamma - 3/v^2, \quad (1.3)$$

where $p^* = p/p_k$; $v = V/V_k$; $\gamma = 1 + 1/c_V$; $c_V = C_V/R_G$; and subscript k denotes the critical values of the thermodynamic parameters, and the subscript 0 the initial values.

Let us also write a dimensionless expression for $(\partial^2 p / \partial V^2)_S$

$$(\partial^2 p^* / \partial v^2)_S = \gamma(\gamma + 1)(p^* + 3/v^2)/(v - 1/3)^2 - 18/v^4.$$

The behavior of the adiabat and the boundary of the domain of anomalous thermodynamic properties is shown in Fig. 1 for $c_V = 20$ (curves 1 and 2, respectively), and $c_V = 30$ (curves 1' and 2'). The boundary of the domain of two-phase states is displayed by the dashed line. It should be noted that single-phase states exist in the domain of anomalous thermodynamic properties only for $c_V > 50/3$.

The dimensionless shock adiabat equation for a van der Waals gas with constant specific heat can be written in the form

$$p^* = [2p_0 c_V (v_0 - 1/3) - p_0 (v - v_0) - 6c_V (v - 1/3)/v^2 + 6c_{V1} (v_0 - 1/3)/v_0^2 + 6(1/v - 1/v_0)] / [2c_V (v - 1/3) + (v - v_0)]. \quad (1.4)$$

It is seen from a comparison of (1.3) and (1.4) that the shock adiabat equation is more complex than the isentropic adiabat equation. However, these adiabats are practically in agreement in the pressure, volume, and specific heat range under consideration. This fact is used below for the foundation of the difference scheme.

2. It is convenient to write the mass, momentum, and energy conservation laws for an arbitrary moving element of the medium through whose boundary there is no material flux in the numerical solution of the problem about dissociation of an arbitrary discontinuity. In the one-dimensional case we have

$$\oint \rho dx = 0; \quad (2.1)$$

$$\oint \rho u dx - p dt = 0; \quad (2.2)$$

$$\oint \rho (E + u^2/2) dx - p u dt = 0 \quad (2.3)$$

(ρ is the density and u is the velocity of the medium). Dissipative terms are not taken into account in (2.2) and (2.3) since the "viscosity" and "heat conductivity" inherent to the difference scheme itself turn out to be of the same order as the real viscosity and heat conductivity for an appropriate selection of the mesh spacings Δx and Δt .

Let us consider an idealized model of a shock tube: A cylindrical tube with closed ends is separated into two compartments, high and low pressure compartments (HPC and LPC), by a baffle. At a certain time the baffle is burst and a compression wave is propagated into the LPC and a rarefaction wave into the HPC. We use the method of Godunov [8] to investigate this process.

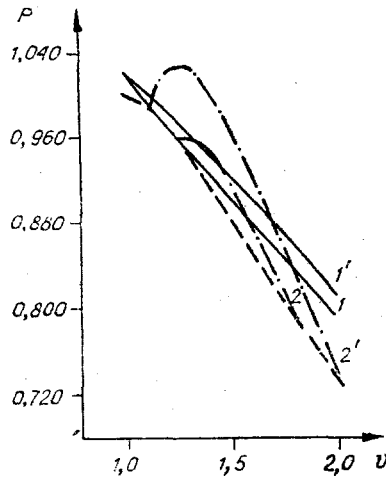


Fig. 1

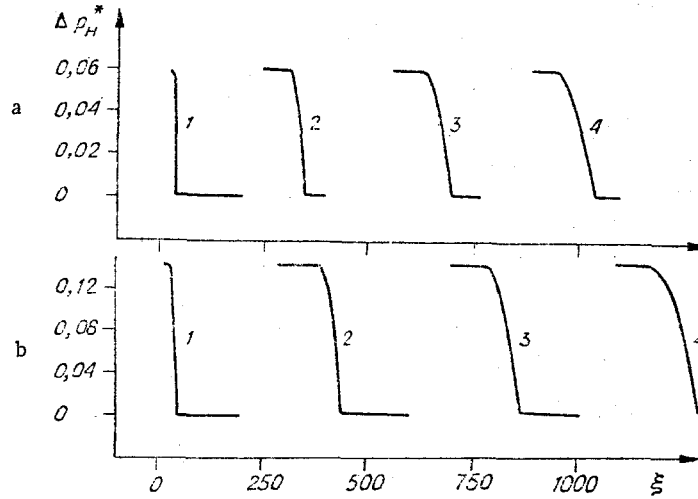


Fig. 2

The difference analogs of (2.1)-(2.3) for the i -th cells can be written in the form

$$\rho'_i \Delta x'_i = \rho_i \Delta x_i (\Delta x_i = x_{i+1} - x_i, x'_i = x_i + \bar{u}_i \Delta t); \quad (2.4)$$

$$\rho_i \Delta x_i (u'_i - u_i) = (\bar{p}_i - \bar{p}_{i+1}) \Delta t; \quad (2.5)$$

$$\rho_i \Delta x_i (E'_i - E_i) = p_i (\bar{u}_i - \bar{u}_{i+1}) \Delta t, \quad (2.6)$$

where x_i and x_{i+1} are coordinates of the cell boundaries (contact discontinuities), \bar{u}_i and \bar{u}_{i+1} are the velocities of the cell boundaries, \bar{p}_i and \bar{p}_{i+1} are the pressures on the cell boundaries. The quantities marked with primes refer to the time $t' = t + \Delta t$. For weak shocks and simple waves, good accuracy in evaluating \bar{u}_i and \bar{p}_i can be obtained by using the "sound approximation" [9]:

$$\bar{u}_i = (p_{i-1} - p_i + a_{i-1}u_{i-1} + a_i u_i) / (a_{i-1} + a_i); \quad (2.7)$$

$$\bar{p}_i = [a_{i-1}a_i(u_{i-1} - u_i) + a_{i-1}p_i + a_i p_{i-1}] / (a_{i-1} + a_i), \quad (2.8)$$

where $a_i = \rho_i c_i$ and c is the adiabatic speed of sound. The use of (2.7) and (2.8) is, moreover, justified in this paper by the agreement, noted above, between the shock and isentropic adiabat.

Therefore, the system of equations (1.1)-(1.2) and (2.4)-(2.8) is mathematically closed and physically founded. The time spacing Δt for a numerical solution is selected in such a manner that the difference scheme would be stable and converge well. The question of the approximation and stability of such a difference scheme is examined in detail in [9].

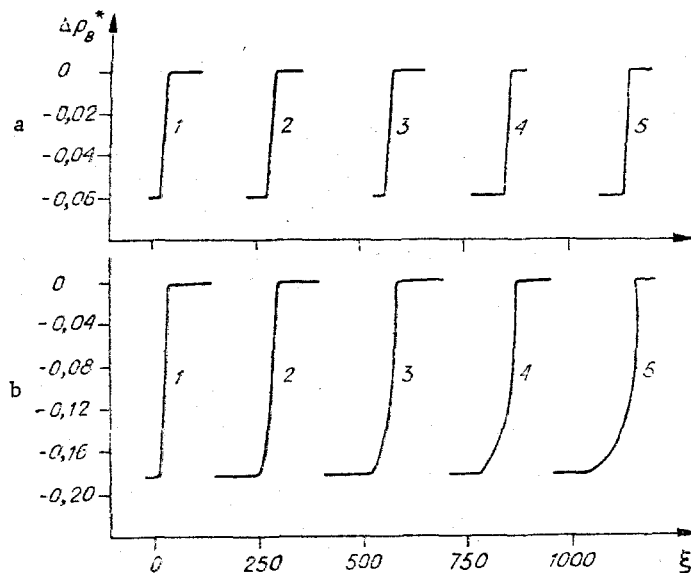


Fig. 3

3. The results of computations are displayed in Figs. 2 and 3. The dimensionless coordinate $\xi = x/\Delta x_0$, where Δx_0 is the initial size of the computational cell, and the dimensionless time $\tau = t/t_*$, where t_* is the characteristic time of the process (the build-up time of the stationary shock profile). The dimensionless pressure perturbation in the compression wave is $\Delta p_L^* = p^* - p_L^*$, and in the rarefaction wave is $\Delta p_h^* = p^* - p_h^*$ (p_L and p_h are the initial pressure in the LPC and HPC, respectively).

Shown in Fig. 2 is the evolution of the compression wave for $cy = 30$; a) the perturbed and unperturbed states are in the domain of anomalous thermodynamic properties (the initial parameters on the discontinuity are the following: $p_L^* = 0.912$, $v_L = 1.54$, $p_h^* = 1.040$, $v_h = 1.11$); b) the unperturbed state is outside this domain ($p_L^* = 0.846$, $v_L = 1.85$, $p_h^* = 1.160$, $v_h = 1.00$); curves 1-4 correspond to the times $\tau = 1; 10; 20; 30$. It is seen from Fig. 2a that the width of the compression wave front increases with time exactly as occurs for a rarefaction wave in an ideal gas. It is shown in Fig. 2b that the leading part of the wavefront corresponding to the domain of normal thermodynamic properties is diffused.

Compression waves with diffused trailing section of the front have been observed only in media with relaxation up to now (the so-called partially dispersed waves) [10]. However, the width of the diffused section remained constant there and was determined by the relaxation time. In the case considered the width of the trailing part of the front is proportional to the path traversed by the wave.

The evolution of a rarefaction wave for $cy = 20$ is shown in Fig. 3; a) the perturbed and unperturbed states are in the domain of anomalous thermodynamic properties (the initial parameters on the discontinuity are the following: $p_L^* = 0.834$, $v_L = 2.00$, $p_h^* = 0.960$, $v_h = 1.25$); b) the perturbed state is outside this domain ($p_L^* = 0.610$, $v_L = 3.33$, $p_h^* = 0.960$, $v_h = 1.25$); curves 1-4 correspond to the same times as in Fig. 2, and curve 5 to $\tau = 40$. It is seen from Fig. 3a that the width of the rarefaction wavefront does not increase with time, i.e., a rarefaction shock holds. It is shown in Fig. 3b that the leading part of the wavefront corresponding to the anomalous thermodynamic properties domain is diffuse. Both these kinds of rarefaction wave configuration have been predicted theoretically [1, 3] and observed in experiment [5, 11].

The data of the computation can be compared with test only qualitatively because the unperturbed state of a substance in the HPC would be very close to the critical state in an experiment. Consequently, the anomalous behavior of the isochoric specific heat [12] apparently played a governing role in tests. Confirmation of this viewpoint might be the fact that the Freon-13 being used in experiment has a "background" (nonanomalous) specific heat $cy \approx 8$ [13], and as had been noted above, rarefaction shocks can exist in a van der Waals gas with constant specific heat, only for $cy > 50/3$.

Therefore, taking account of the anomalous behavior of the specific heat near the fluid-vapor critical point should result in significant expansion of the class of substances in which rarefaction shocks can be propagated. Moreover, the results should not change qualitatively if a scale equation of state is used instead of the van der Waals equation.

4. Let us compare the results obtained with the data on wave propagation in solids experiencing polymorphic transformation. Fragments with a smooth surface were observed in [14-16] during explosive loading of iron and steel specimens. This phenomenon is explained by the interaction of the rarefaction shocks. The existence of a rarefaction shock in solids experiencing polymorphic transformations is related to the fact that the presence of the phase transition results in the appearance of a section with convexity upward on the adiabat, i.e., a section on which the mean value of the second derivative of the pressure with respect to the volume for constant entropy is less than zero. The rarefaction wave profile consisting of the shock and the subsequent simple wave is presented in [16]. An analogous rarefaction wave structure is obtained in this paper.

As regards the compression wave, in solids experiencing polymorphic transformations they are always propagated in the form of shocks (one or two). Compression waves consisting of a shock and a diffuse trailing part of the front which are possible near the fluid-vapor critical point cannot be observed in solids. This is because at all points in solids where the adiabat has no singularities, $(\partial^2 p / \partial V^2)_S > 0$ [1].

Therefore, the similarity of processes occurring in solids experiencing polymorphic transformations, and near the fluid-vapor critical point, is related to the anomalous behavior of the adiabat, while the distinction is associated with the different physical nature of this anomaly. If this is a phase transition in solids, then near the critical point it is a strong change in the thermodynamic properties (compressibility, etc.) of a single-phase substance.

The authors are deeply grateful to Ya. B. Zel'dovich and V. E. Nakoryakov for interest in this research and for critical remarks.

LITERATURE CITED

1. Ya. B. Zel'dovich and Yu. P. Raizer, Physics of Shock Waves and High-Temperature Hydrodynamic Phenomena [in Russian], Nauka, Moscow (1966).
2. Ya. B. Zel'dovich, "On the possibilities of rarefaction shocks," Zh. Eksp. Teor. Fiz., 16, No. 4 (1946).
3. B. L. Rozhdestvenskii and N. N. Yanenko, Systems of Quasilinear Equations and Their Application in Gasdynamics [in Russian], Nauka, Moscow (1978).
4. A. A. Borisov, "Evolution of finite perturbations near the fluid-vapor critical point," Dokl. Akad. Nauk SSSR, 255, No. 1 (1980).
5. S. S. Kutateladze, Al. A. Borisov, et al., "Experimental detection of rarefaction waves near the fluid-vapor critical point," Dokl. Akad. Nauk SSSR, 252, No. 3 (1980).
6. G. Stanley, Phase Transitions and Critical Phenomena [Russian translation], Mir, Moscow (1973).
7. L. D. Landau and E. M. Lifshits, Statistical Physics [in Russian], Pt. 1, Nauka, Moscow (1976).
8. S. K. Godunov, "Difference method of numerical computation of discontinuous solutions of the hydrodynamics equations," Mat. Sb., 19, No. 3 (1959).
9. S. K. Godunov, ed., Numerical Solution of Multidimensional Gasdynamics Problems [in Russian], Nauka, Moscow (1976).
10. E. Becker, "Relaxation effects in gas flow," Fluid Dyn. Trans., 7, Pt. 1 (1974).
11. Al. A. Borisov and A. A. Borisov, "Rarefaction wave dynamics in a substance in the critical domain of a fluid," in: S. S. Kutateladze (editor), Investigations on Hydrodynamics and Heat Exchange [in Russian], Inst. Thermophys., Siberian Branch, Acad. Sci. of the USSR, Novosibirsk (1980).
12. M. A. Anisimov, "Investigations of critical phenomena in fluids," Usp. Fiz. Nauk, 114, No. 2 (1974).
13. V. F. Tomanovskaya and B. E. Kolotova, Freons. Properties and Application [in Russian], Khimiya, Leningrad (1970).
14. J. O. Erkmann, "Smooth spalls and the polymorphism of iron," J. Appl. Phys., 32, No. 5 (1961).

15. A. G. Ivanov and S. A. Novikov, "On rarefaction shocks in iron and steel," Zh. Eksp. Teor. Fiz., 40, No. 6 (1961).
16. A. G. Ivanov, S. A. Novikov, and Yu. I. Tarasov, "Spalling phenomena in iron and steel caused by rarefaction shock interaction," Fiz. Tverd. Tela, 4, No. 1 (1962).

DETONATION OF A PHLEGMATIZED EXPLOSIVE

L. V. Al'tshuler, V. V. Balalaev,
G. S. Doronin, V. S. Zhuchenko,
and A. S. Obukhov

UDC 662.215.12-398

It is common to use explosives containing inert organic additives as binding or phlegmatizing agents. However, not much is known about the effects of these components on the detonation characteristics. Most papers give the detonation speeds of the mixtures [1-3], while the information on the pressure of the explosion products is limited and conflicting. For example, according to some sources [4] mixing an explosive with wax increases the detonation pressure, while other sources [5, 6] quote the opposite result.

We have used manganin transducers to identify the major features in the detonation of hexogen and TEN containing 6% of macromolecular compounds of the paraffin series.

Detonation waves with planar fronts are produced in charges of these materials, and also in trotyl, in each case of diameter 64 mm. In certain experiments the charge diameter was 84 mm. The ends of the charges were formed by materials differing in dynamic rigidity: copper, aluminum, Plexiglas, and ethanol. The flat manganin transducers were insulated from the electrically conducting medium by layers of PTFE joined together with vacuum lubricant, and these were placed within the charge or at the boundary between the explosive and the end. The signals were recorded with an S1-75 oscilloscope and the pressure profile $p(t)$ was determined from the calibration relationship of [7]. The detonation speed was measured with electrical contacts with an error of $\pm 0.5\%$.

Figure 1 shows $p(t)$ recorded with the manganin transducers for phlegmatized TEN of density $\rho = 1.655 \text{ g/cm}^3$. Line 1 was recorded with the transducer inserted directly in the explosive at a distance 120 mm from the initiation surface. Line 2 characterizes the pressure change at the same distance from the boundary with an aluminum plate. Figures 2 and 3 show analogous curves respectively for phlegmatized hexogen ($\rho = 1.66 \text{ g/cm}^3$) and for trotyl ($\rho = 1.56 \text{ g/cm}^3$) with the same geometry. Lines 1 relate to the pressure within the charge, while lines 2 relate to the pressure at the boundary with the Plexiglas. The fluctuations in the first 0.15-0.25 μsec correspond to wave reverberations in the insulation and in the transducer itself.

Figures 1 and 2 show that the phlegmatized explosives have a horizontal part in the initial stage. Special experiments showed that the length of the plateau, behind which there is a fall in pressure, increases with the length of the charge and constitutes about 1 μsec in hexogen for $L = 120 \text{ mm}$.

Table 1 gives the initial density ρ , detonation speed D , observed plateau pressure within the explosion products EP within the charge, and the same at the boundaries with copper, aluminum, Plexiglas (P1), and ethanol (et). The bottom lines in the entries for the experimental pressures are the numbers of experiments used in the averaging.

We constructed the retardation and expansion branches for the EP from these experimental results in terms of a plot of pressure p against mass velocity u . The detonation pressure p^* in the last column of Table 1 was determined from the point of intersection of these curves with the detonation ray $p = \rho Du$; this column also gives in parentheses the published data on the pure explosives.

Table 1 shows that 6% phlegmatizer substantially reduces the detonation pressure. On the other hand, the detonation speed is not reduced and even increases somewhat. For ex-